AAEC/TM573

AUSTRALIAN ATOMIC ENERGY COMMISSION

RESEARCH ESTABLISHMENT
LUCAS HEIGHTS

keV NEUTRON CAPTURE IN ZINC

by

B.J. ALLEN
A.R. de L. MUSGROVE

November 1970

ISBN 0 642 99395 5

AUSTRALIAN ATOMIC ENERGY COMMISSION

RESEARCH ESTABLISHMENT

LUCAS HEIGHTS

keV NEUTRON CAPTURE IN ZINC

by

B. J. ALLEN

A. R. de L. MUSGROVE

ABSTRACT

Averaged gamma ray transition strengths in ^{65}Zn and ^{67}Zn have been measured after neutron capture in the keV energy region. These results have been compared with calculations based on resonance parameters and a statistical neutron capture mechanism.

Evidence for d-wave capture in excess of that expected is given. However, because of the substantial deviation from statistical behaviour of the averaged transition strengths, it is apparent that configuration effects play a major role in the determination of partial capture cross sections.

National Library of Australia card number and ISBN 0 642 99395 5

CONTENTS

continued...

1. INTRODUCTION

The quantitative study of averaged resonance neutron capture in the keV energy range requires a detailed knowledge of the spins and parities of the final states (J_f^π) and a close resonance spacing to ensure good averaging for the random matrix elements. The measured average partial radiative widths $\langle\gamma_{if}\rangle$ can then be related to:

(a) the energy dependence and ratio of electric and magnetic multipole transition strengths,

(b) the magnitude of the s, p and d-wave capture cross sections, and

(c) the neutron capture mechanism and configuration effects.

Results have been reported for keV averaged capture in copper and nickel (Allen et al. 1968, 1969) which indicate an E_γ^3 gamma ray energy dependence of E1 partial widths. This result is characteristic of a statistical capture mechanism with a constant average partial cross section. However the results remain only qualitative because of the lack of J_f^π assignments for copper and the wide resonance spacing in nickel.

In averaged measurements in the eV region Bollinger and Thomas (1968) have found for erbium a banding of $\langle\gamma_{if}\rangle$ to final states of different J_f^π. From this, estimates of the ratio of E1, M1 and E2 averaged transition strengths were obtained. These results indicate that the configurations of the capture and final states play a minor role in the determination of the averaged transition strengths for this nucleus.

In an endeavour to obtain more quantitative results in the keV region for light nuclei, capture gamma ray spectra in zinc have now been measured. Reasonable averaging can be achieved with zinc 64 because the s-wave resonance spacing is about 2.5 keV, and many low lying states in ^{65}Zn have definite spin and parity assignments.

In this report preliminary experimental results and interpretation are presented. A closer investigation is being made of the keV capture mechanism for nuclides in this mass region.

2. MEASUREMENT AND ANALYSIS

The experimental arrangement was similar to that described previously (Allen et al. 1969). A pulsed proton beam incident on a lithium target permitted time of flight selection of neutron capture events in the keV energy region (Figure 1). The total time jitter of the system was approximately 30 ns and the resolution of a 30 cm^3 Ge(Li) detector was 10 to 20 keV for 7 MeV gamma rays, depending on the total count rate.

The detector was shielded by a B_4C-paraffin cone placed at 0° in the proton

beam direction and in the centre of a curved annular target of natural zinc. The target (weight 31 kg) was placed 50 cm from the Li(p,n) neutron source, and was irradiated for approximately 60 hours.

An on-line computer was used to analyse time-of-flight and gamma ray energy data in coincidence, using the digital window technique (Allen et al. 1968). Five time-of-flight windows were set, four to select fast neutron capture events and one to sample the background (assumed to be time independent). The normalised background was subtracted from the keV spectra and the results are shown in Figure 2. Broadening of the gamma ray peaks occurs in the higher neutron energy windows as a result of the neutron energy spread.

It is apparent that the keV spectra are much more complex than the thermal spectrum, which includes a small background component due to iron (present in the concrete floor). Further, the intensities and energies of the keV capture gamma rays change substantially as neutron energy increases. The high energy parts of these spectra were analysed by least squares methods with the on-line computer (Allen et al. 1968) (see Table 1).

To obtain an averaged result over the entire neutron energy range, the spectra are shifted in energy by an amount equal to the average neutron energy for each window, then summed and corrected for detector efficiency (Figure 3). The gamma ray energies are then equivalent to those observed in thermal capture and a direct comparison can be made with (d,p) levels (Von Ehrenstein and Schiffer 1967) and thermal intensities (Bartholomew et al. 1967) (see Table 2).

The neutron energy range covered by the sum spectrum is approximately 60 keV, and encompasses at least 24 s-wave resonances. The s-wave contribution to the gamma ray intensities therefore represents average values with a standard deviation of about 30 per cent, given by a chi-squared distribution with 24 degrees of freedom.

3. CALCULATIONS

3.1 Averaged ℓ-wave Cross Sections

In the energy range 10-100 keV, significant contributions to the capture cross section are expected from neutrons with angular momentum up to $\ell = 2$. The individual ℓ-wave capture cross sections can be calculated when the average properties of the resonances and their distributions are known and a statistical capture mechanism is assumed.

Generally, knowledge of these parameters is restricted to s-wave resonances only, while p- and d-wave parameters are sparse. The best available resonance parameters for ^{65}Zn are summarised in Table 3. On the basis of these measured and interpolated data, ℓ-wave capture cross sections for ^{64}Zn + n have been

calculated (Musgrove 1969). Figure 4 gives calculated cross sections for the zinc isotopes and compares them with the natural zinc cross section tabulated by Macklin and Gibbons (1965). Also shown are the p- and d-wave contributions to the ^{65}Zn cross section.

The calculated cross sections are too high at high energies, the discrepancy being almost entirely due to the assumed d-wave contribution to the cross sections. At 100 keV, this d-wave estimate alone would be about twice the measured cross section. The best fit to experiment is given with a zero d-wave cross section.

It remains now to estimate the dependence of the averaged partial widths on these cross sections and on the spins and parities of the final states.

3.2 Gamma Ray Spectra

In the statistical decay of the compound nucleus, the observed gamma ray intensity for any transition between the capture states i, and a particular final state f, can be written as a sum of terms corresponding to each electric and magnetic multipole transition from s-, p-, and d-wave resonances. Each term is normalised to the predicted ℓ-wave capture cross section and a number of equations are then obtained for the expected statistical transition strength to each final state of specified J^{π}. We have ignored quadrupole and higher order transitions and have assumed a constant ratio between electric dipole and magnetic dipole partial widths:

$$\langle\gamma(M1)\rangle/\langle\gamma(E1)\rangle = \beta \quad .$$

Bartholomew (1961) in a survey of thermal capture transitions showed that the average E1 strength is an order of magnitude stronger than that for M1 and in these calculations the value of β was varied from 10^{-2} to unity.

The capture cross section for ℓ-wave neutrons into a final state of spin J is given by:

$$\sigma_{J\ell} = \frac{2\pi^2}{k^2} \langle\Gamma_\gamma\rangle S_\ell P_\ell \sqrt{E}\, g_J \frac{\epsilon^{\ell}_{IJ} F(\alpha_{\ell J})}{\langle\Gamma_J\rangle} \quad , \qquad \ldots(1)$$

where the symbols have their conventional meanings (Musgrove 1969, 1970). The relative transition intensity between the capturing state J_i and a particular final state J_f is:

$$I_{if} = \sigma_{J\ell} \cdot \frac{\gamma_{if}}{\Gamma_\gamma} \quad , \qquad \ldots(2)$$

where γ_{if} = partial radiative width between initial and final state,

and

$$\Gamma_\gamma = \sum_{\text{final states}} \gamma_{if} \quad .$$

From statistical region capturing states at energy E, the total transition strength to the final state,

$$I_f \propto \sum_{\ell=0}^{\ell=2} \sum_{J_i=||I-\ell|-\frac{1}{2}|}^{I+\ell+\frac{1}{2}} \sigma_{J\ell} \cdot \left[\frac{\epsilon(J_i,J_f)\ E_{if}^{\ 3}}{T_{\ell Ji}} \right] , \qquad \ldots(3)$$

where $E_{if}^{\ 3}$ = electromagnetic form factor,

$T_{\ell Ji}$ is a normalisation factor given by

$$T_{\ell Ji} = \sum_{J_f}^{\text{all transitions}} E_{if}^{\ 3}\ \epsilon(J_i,J_f) ,$$

and $\epsilon(J_i,J_f)$ = 1 if decay proceeds via E1 transition
= β if decay proceeds via M1 transition
= 0 otherwise.

For capture in ^{64}Zn, Table 4 gives the electromagnetic decay scheme from the possible capturing states to six final states with different J^{π} assignments. Line intensities for the transitions to final states with spin assignments 5/2-, 1/2-, 5/2+ and 1/2+, relative to the 3/2- transition are evaluated at 10, 30 and 50 keV for β values of 10^{-2}, 10^{-1} and 1. The 3/2- transition is seen from Table 4 to be the strongest line of the statistical spectrum, provided p-wave capture is unimportant compared with s-wave capture.

In Figure 5 we show the results of two different calculations. The first assumes a cross section for ^{64}Zn + n which includes a d-wave contribution (the parameters of Table 3) while the second assumes a zero d-wave strength function which gives a calculated cross section more in accord with the natural zinc cross section data.

The calculated line intensities with d-wave contribution included show an order of magnitude increase in the ground state transition (5/2-) over the intensity calculated for no d-wave contribution.

The spin assignment of the 1.370 MeV level is uncertain and if the spin is 3/2+, reference to Table 4 shows that the relative transition intensity to this state will be much the same as that to the 1/2+ final state.

4. DISCUSSION

4.1 d-Wave Capture

Perhaps the most important feature of the observed averaged transition strengths

is the strong intensity of transitions leading to the 5/2- ground states in ^{65}Zn and ^{67}Zn. Two alternative explanations in terms of the statistical decay of the compound nucleus are possible.

(a) p-wave capture followed by M1 (or E2) transitions

Estimates of the p-wave strength function show considerable variation in this mass region. Hockenbury (1967) and Morgenstern (1968) obtained estimates which range from 0.5×10^{-4} to 0.04×10^{-4} $(eV)^{-\frac{1}{2}}$. Musgrove (1969) had difficulty fitting measured cross sections in this region with p-wave strength functions much above 0.02×10^{-4} $(eV)^{-\frac{1}{2}}$. Figure 4 clearly demonstrates that if the d-wave cross section is ignored, a p-wave strength function which is only a factor of three greater than that assumed would result in the calculated cross sections being systematically too high at high energies.

If we assumed a value for β of 0.1, it would be impossible on statistical considerations alone, to account for the observed ground state line intensity. An order of magnitude increase in the p-wave strength function would certainly increase the 5/2- intensity, but would also lead to a domination of the calculated spectrum by the lines to positive parity final states which are fed by E1 transitions from p-wave capturing states. This clearly does not occur. The averaged intensity for the ground state transition in keV capture is at least a factor of two greater than the intensity of the 1/2+ transition.

(b) d-wave capture followed by E1 transitions

The predicted strength of the gamma ray transition to the 5/2- ground state becomes significant when a d-wave contribution to the cross section is included. Figure 5 shows that the predicted average intensity of this line up to ~ 50 keV relative to the 1/2- or 3/2- transitions is of the order of 2:9, while it should be larger by a factor of ~ 2 than the transition to the 1/2+ final state.

The averaged intensity measurements of Table 2 indicate a ratio for the ground state transition relative to the 1/2- transition of ~ 1:2 while its strength is comparable with that to the 3/2- state.

The intensity of the 5/2- transition relative to the 1/2+ transition has an upper limit somewhat larger than predicted, but the actual 1/2+ strength is obscured by two neighbouring transitions. The observed transition to the state (3/2+, 5/2+) is a factor of three smaller than the averaged ground state intensity.

The qualitative predictions of the statistical theory with a d-wave capture component in the cross section are reasonably well confirmed by the experimental results. Nevertheless a number of deviations exist. The most striking one is, of course, the anomalous behaviour of the strengths to 1/2- and 3/2- final states. This is discussed more fully in the next section.

The problem with the experimental cross section still remains, of course, but it is not unknown for two measured cross sections to differ by more than the discrepancy between our calculations and the experimental data, particularly for the higher energy regions. We do not regard this discrepancy as serious (at present) in view of the confirming evidence of this experiment.

This anomalous result is similar to that observed by Bergqvist et al. (1967) in the mass region $20 < A < 40$ and Harvey et al. (1964) for $90 < A < 140$. Both mass regions correspond to peaks in the p-wave strength function, resulting from 2p and 3p shell states. It is not surprising, therefore, that in the mass region $50 < A < 70$, a strong influence on neutron resonances exists not only for the 3s neutron shell but also the 2d shell.

4.2 Ratio of $p\frac{1}{2}$ and $p\frac{3}{2}$ Strengths

In both ^{65}Zn and ^{67}Zn the average strength for transitions to the first 1/2- state is greater than that to the first 3/2- state. The ratio decreases with increasing neutron energy as would be expected from an increasing d-wave contribution. However, it is not possible to obtain the experimental result using the theory of Section 3, and it is therefore evident that a non-statistical process is important here.

4.3 Positive Parity States

The observation of significant transition strengths to 1/2+ and 5/2+ states is in better accord with the calculations of Section 3. For $\langle\gamma(M1)\rangle/\langle\gamma(E1)\rangle = 0.1$, a p-wave strength function only slightly larger than the 0.01×10^{-4} $eV^{-\frac{1}{2}}$ assumed would be sufficient to account for the transition strengths to these states.

The calculated strengths are relatively independent of the magnitude of the d-wave cross section, and are most sensitive to neutron energy. However, the experimental data are insufficient to permit any conclusions to be drawn.

4.4 Correlations of Reduced Widths: keV, thermal, (d,p)

The above explanation of the results in terms of a statistical capture mechanism is only partly satisfactory. Such an analysis assumes a complex capture state and does not take into account the final state configurations.

We now extend the discussion to include data from both thermal capture and the (d,p) reaction.

(a) Reduced widths

The (d,p) reaction selects final states with strong single particle components. The neutron transfer reaction is analogous to capture and it is therefore useful to compare reduced neutron widths with thermal and keV capture matrix elements.

Von Ehrenstein and Schiffer (1967) have obtained reduced neutron widths for

^{65}Zn, that is $(2J_f + 1)S$, where S is the spectroscopic factor. Gamma ray matrix elements are obtained after reducing intensities by an E_γ^3 factor. In the case of keV capture, a correction is also required for the spin and parity of the final states and the relative ℓ-wave cross sections. However in view of the substantial deviation from statistical behaviour, this correction has not been made.

Reduced widths for (d,p) thermal and keV capture are shown in Figure 6, normalised to the second excited state strength. As only s-wave capture is possible in the thermal case, El reduced widths should be compared only with $\ell_n = 1$ neutron widths. However, this is not so in keV capture.

Figure 6 shows that for $\ell_n = 1$ the thermal capture reduced widths fall off rapidly with excitation energy. The keV results, however, remain approximately constant, and a least squares fit of the keV intensities over an energy range of $2\frac{1}{2}$ MeV yields an $E_\gamma^{3.9}$ energy dependence. This result is somewhat greater than that obtained for copper and nickel (Allen et al. 1968, 1969) and the E_γ^3 energy dependence included in the statistical calculations.

(b) 5/2- ground state

It is evident from the (d,p) assignments that the major part of the $\ell_n = 3$ strength must be present in the 5/2- ground state. El transitions to this state are possible only after d-wave capture and the experimental result has been found to indicate a large d-wave capture cross section (Section 4.1).

If it is assumed that most of the d-wave capture decays through the ground state for configuration reasons, then the required cross section is reduced by a factor of four, and is approximately that shown in Figure 4 (that is, a strength function of about 2×10^{-4} $eV^{-\frac{1}{2}}$).

(c) 1/2- first excited state

If thermal capture is predominantly a single particle reaction, then a correlation is expected between those final states with large reduced neutron widths in the (d,p) reaction and the strongest gamma ray matrix elements in the thermal capture. While agreement is good for the 3/2- second excited state, no thermal transition has ever been observed to the 1/2- first excited state. This lack of correlation has been discussed by Groshev and Demidov (1967) together with two other cases in ^{57}Fe and ^{63}Ni, and it suggests strong configuration effects. The keV result is in better agreement with the reduced neutron width and it is apparent that different configurations must apply in the keV case.

The thermal capture cross section of ^{64}Zn is relatively low, and because of the substantial difference in spectra, is probably the result of 'between resonance' capture. However, it should be noted that this experiment is not sensitive to neutron resonances below about 5 keV and the influence of this energy region on the thermal capture reaction remains uncertain.

(d) Isotonic nuclei: ^{63}Ni and ^{65}Zn

To understand the gamma ray spectra of ^{65}Zn it is necessary to consider the shell model configurations of this nucleus and that of its isotone ^{63}Ni. The centroid energies of single particle states are found to be comparable in these isotones (Lin and Cohen 1963). However, substantial changes in energies occur with neutron number (Cohen et al. 1963) and a large overlap of the $p\frac{3}{2}$ and $f\frac{5}{2}$ shells is expected in this mass region. The ground state configurations of the target nuclei, ^{62}Ni and ^{64}Zn, therefore remain uncertain.

In the discussion of the ^{63}Ni anomaly, Groshev and Demidov (1967) have assumed a ground state neutron configuration for ^{62}Ni of $p\frac{3}{2}^2\ f\frac{5}{2}^4$. Our interpretation of the ^{65}Zn data also requires this configuration for the ground state of ^{64}Zn. The relevant transitions and configurations for these nuclei are illustrated in Figure 7, together with the relative intensities of the thermal and keV capture gamma rays.

In ^{63}Ni, the excitation of a two particle capture state is required for a qualitative explanation of the observed transition strengths, and it is probable that this state is the lowest energy resonance at 4.6 keV which is thought to influence the thermal capture reaction (Allen et al. 1969). For a capture resonance to have such a simple configuration is unexpected, and the properties of this resonance therefore warrant further investigation.

There is no evidence for a resonance dominating thermal capture in ^{64}Zn, and it may be assumed that a direct capture process as described by Lane and Lynn (1960) occurs with the only suitable final state for a single particle transition being the 3/2- second excited state.

In the low keV region, the resonance configurations may be sufficiently complex to permit transitions to many final states. However, configuration effects appear to remain significant up to neutron energies of about 50 keV.

4.5 Isotopic Cross Sections

The intensities of the transitions to the ground and first three excited states in ^{65}Zn and ^{67}Zn are very similar. If these four gamma rays occur in the same proportion to the total number of captures, then the sum of their intensities can be corrected for abundances to give the ratio of the capture cross sections, that is,

$$\sigma(^{64}\mathrm{Zn}) = (1.2 \pm 0.3)\ \sigma(^{66}\mathrm{Zn}) \quad .$$

The near equality of these cross sections at 30 keV suggests that the extra neutron pair in ^{66}Zn has little effect, in contrast to the results obtained for the nickel isotopes (Allen et al. 1969) where the cross sections approximately doubled for each additional neutron pair.

5. ACKNOWLEDGEMENTS

The authors acknowledge the cooperation of members of the 3 MeV accelerator group at Lucas Heights. The Ge(Li) detector was prepared by A. J. Tavendale and A. C. Dawson. H. G. Broe and M. D. Scott assisted in the fabrication and development of the cryostat.

6. REFERENCES

Allen, B. J. (1968). - Nuc. Phys. A111:1.

Allen, B. J., Kenny, M. J. and Sparks, R. J. (1969). - Nuc. Phys. A122:220.

Allen, B. J., Upex, G. D. and Trimble, G. (1968). - AAEC/TM458.

Bartholomew, G. A. (1961). - Am. Rev. Nucl. Sci. 11:259.

Bartholomew, G. A., Doveika, A., Eastwood, K. M., Monaro, S., Groshev, L. V., Demidov, A. M., Pelekhov, V. I. and Sokolovskii, L. L. (1967). - Nuclear Data, (A)3:544.

Bergqvist, J. A., Biggerstaff, J. H., Gibbons, J. H. and Good, W. M. (1967). - Phys. Rev. 158:1049.

Bollinger, L. M. and Thomas, G. E. (1968). - Phys. Rev. Lett. 21:233.

Cohen, B. L., Fulmer, R. H., McCarthy, A. L. and Mukherjee, P. (1963). - Rev. Mod. Phys. 35:332.

Groshev, L. V. and Demidov, A. M. (1967). - Sov. Jour. Nuc. Phys. 4:558.

Harvey, J. A., Slaughter, G. G., Bird, J. R. and Chapman, G. T. (1964). - ORNL-3582.

Hockenbury, R. W. (1967). - Ph.D. Thesis, Rensselaer Polytechnic Inst.

Lane, A. M. and Lynn, J. E. (1960). - Nuc. Phys. 17:563.

Lin, E. K. and Cohen, B. L. (1963). - Phys. Rev. 132:2632.

Macklin, R. L. and Gibbons, J. H. (1965). - Rev. Mod. Phys. 37:166.

Morgenstern, J. (1968). - CEA-R-3609.

Musgrove, A. R. de L. (1969). - AAEC/E198.

Musgrove, A. R. de L. (1970). - AAEC/E198 Supplement.

von Ehrenstein, D. and Schiffer, J. P. (1967). - Phys. Rev. 164:1374.

TABLE 1

VARIATION OF RELATIVE GAMMA RAY INTENSITIES FOR

^{65}Zn and ^{67}Zn WITH NEUTRON ENERGY

Digital Window		DW1	DW2	DW3	DW4
Average Neutron Energy (keV)		5	11	27	49
	Zinc 65				
Transition Intensities Relative to γ_2	γ_0	1.0	0.8	0.9	0.8
	γ_1	3.0	2.0	1.7	0.8
	γ_2	1.0	1.0	1.0	1.0
	γ_3	1.0	1.0	1.0	0.8
*Unresolved Transitions	γ_4	1.0	*	*	0.7
	Zinc 67				
	γ_0	0.3	*	*	1.9
	γ_1	0.7	1.1	*	4.2
	γ_2	1.0	1.0	*	1.0

TABLE 2

AVERAGED GAMMA RAY INTENSITIES IN ZINC

Zinc 65	E_f	J_f	ℓ_n	$E_\gamma^{(1)}$ (d,p)	$E_\gamma^{(2)}$ Thermal	$I_\gamma^{(3)}$	(4)	$\langle I_\gamma \rangle^{(5)}$ keV
0	0.0	5/2-	3	7,988	-			0.9
1	54	1/2-	1	7,934	-			1.5
2	115	3/2-	1	7,873	7,863	11.70	$\gamma_4^{(68)}$	< 1.0
3	205	(3/2-)	1	7,783	-			0.8
4	865	1/2-	1	7,123	7,112	1.61		0.4
5	908	1/2-, 3/2-	1	7,080	7,069	1.61		
6	1,064	9/2+	4	6,924				
7	1,370	(3/2+, 5/2+)	2	6,618				0.3
8	1,469	1/2-, 3/2-	1	6,519	6,509	0.91	$\gamma_0^{(68)}$	< 0.5
9	1,911	1/2+	0	6,077			$\gamma_5^{(67)}$	< 0.3
10	2,054	-	-	5,934			$\gamma_6^{(67)}$	
11	2,421	1/2-, 3/2-	1	5,567	5,560	1.06		
12	2,491	1/2+	0	5,497				
13	2,532	(5/2)+	2	5,456				0.3
14	2,375	-	-	5,413	5,405	0.13		
15	2,674	(5/2)+	2	5,314				
Zinc 67								
0	0.0	5/2-	3	7,053			$\gamma_5^{(65)}$	< 1.0
1	93	1/2-	1	6,960	6,959	3.21		1.6
2	184	3/2-	1	6,869	6,868	2.02		1.0
3	390	3/2-	1	6,663	6,658	1.22		1.0
4	602	9/2+	4	6,451				
5	978	(5/2)+	2	6,075				
6	1,142	1/2-	1	5,911	5,910	1.00		
7	1,444	3/2-	1	5,609				
8	1,542	1/2-, 3/2-	1	5,511	5,521	0.39		
9	1,642	-	-	5,411	5,405	0.13		
10	1,676	1/2+	0	5,377				

(1) From (d,p) data assuming a binding energy of 7,988 keV (Bartholomew et al. 1967)

(2) 10 keV systematic error between thermal energies (Bartholomew et al. 1967) and (d,p) levels (V. Ehrenstein and Schiffer 1967).

(3) Intensity per 100 captures in natural zinc

(4) Unresolved isotopic transitions

(5) Relative to I_2, (± 20%) for $(E_n) \sim 30$ keV

TABLE 3

RESONANCE PARAMETERS FOR ZINC 64

Parameter	Measured	References	Footnotes	Adopted in Cross Section Calculation
$\langle D \rangle$ keV	2.5	1		2.0
Γ_γ eV	0.3	1	*	0.55
$S_0 \times 10^4 \ (eV)^{-\frac{1}{2}}$	2.3	2	‡	2.3
$S_1 \times 10^4 \ (eV)^{-\frac{1}{2}}$	< 0.25	3	†	0.01
$S_2 \times 10^4 \ (eV)^{-\frac{1}{2}}$	2.00 ± 1.00	3	†	2.00

1. Goldberg, M. D., Mughabghab, S. F., Magurno, B. A. and May, V. M. (1966). - Neutron Cross Sections - BNL325, 2nd Edition, Supp. No. 2, Vol. IIA.

2. Cote, R. E., Bollinger, L. M. and le Blanc, J. M. (1958). - Phys. Rev. 111:288.

3. Seth, K. K., Tabony, R. H., Bilpuch, E. G. and Newson, H. W. (1964). - Phys. Lett., 13:70.

* Based on first resonance only (but Kim et al. (1965) - Zhur Eksp i Teoret Fiz 49, 410 give 0.670 eV).

‡ Value of 1.1 given in a private communication from J. A. Biggerstaff and R. Farrell to K. K. Seth. In any case the s-wave cross sections are approximately independent of this parameter.

† Values given for natural zinc.

TABLE 4

DECAY SCHEME FROM POSSIBLE CAPTURE STATES TO

FINAL STATES WITH SIX DIFFERENT SPIN ASSIGNMENTS

Capturing State	Spin Weight Factor	Final States MeV Energies					
		0 5/2-	0.54 1/2-	0.115 3/2-	1.370 5/2+	1.370 3/2+	1.911 1/2+
s 1/2+	1	M2	E1	E1	E2	M1	M1
p 1/2-	1/3	E2	M1	M1	M2	E1	E1
p 3/2-	2/3	M1	M1	M1	E1	E1	E1
d 3/2+	2/5	E1	E1	E1	M1	M1	M1
d 5/2+	3/5	E1	M2	E1	M1	M1	E2

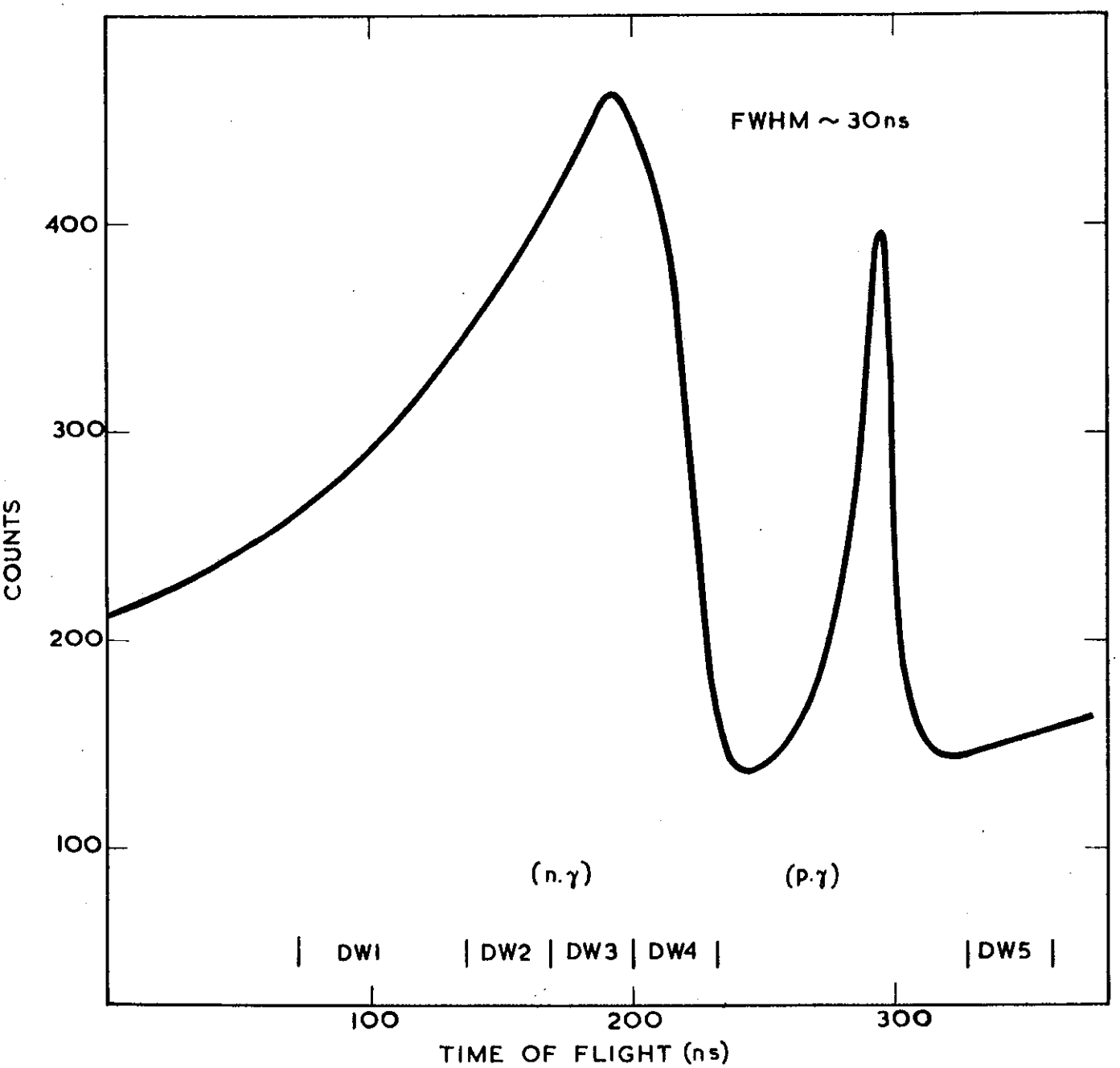

FIGURE 1. TIME-OF-FLIGHT SPECTRUM

Digital windows are set to encompass keV capture events and to sample the time-independent background.

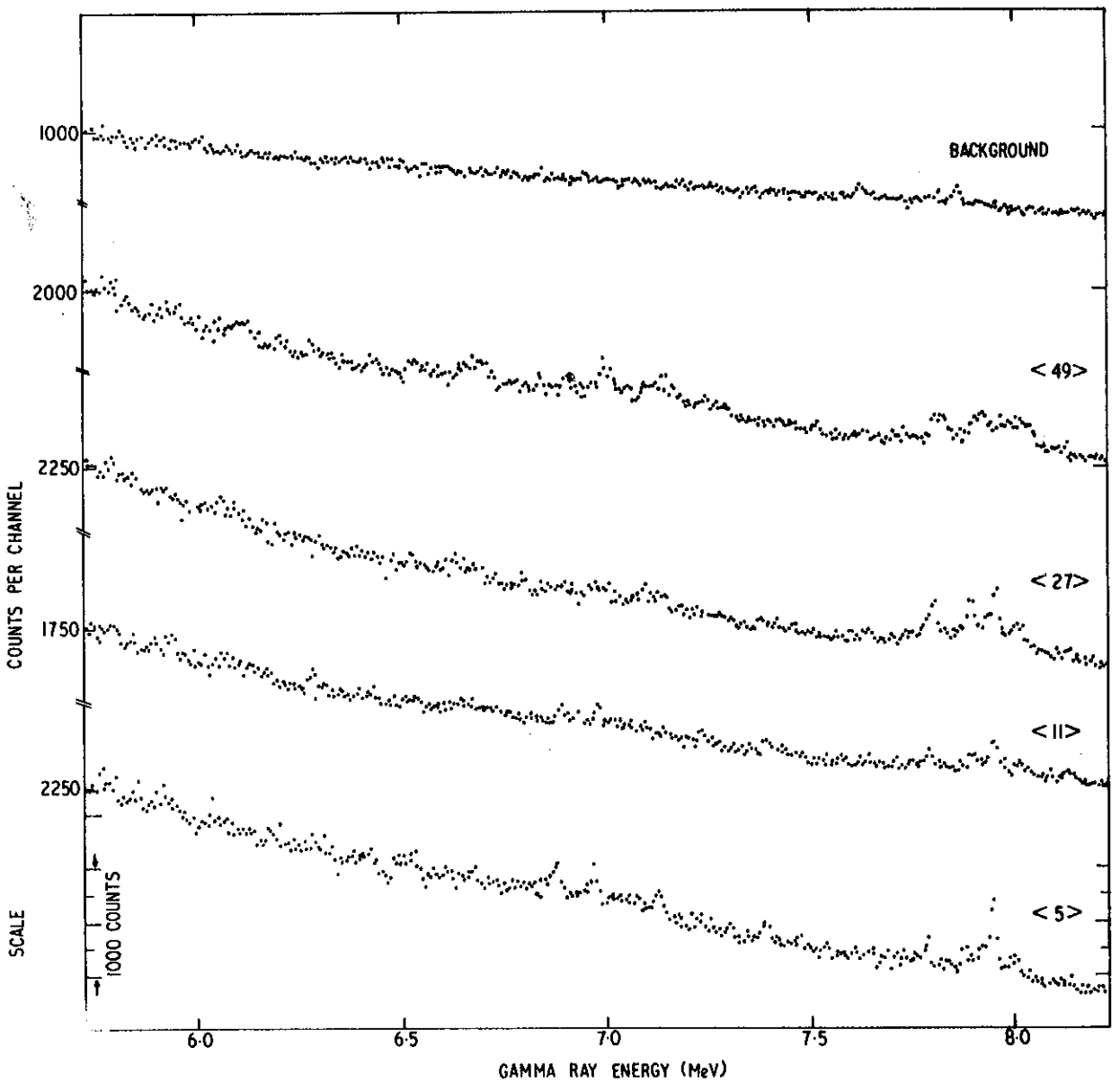

FIGURE 2. CAPTURE SPECTRA FROM ZINC

Background subtracted spectra are shown for each digital window, together with the background spectrum

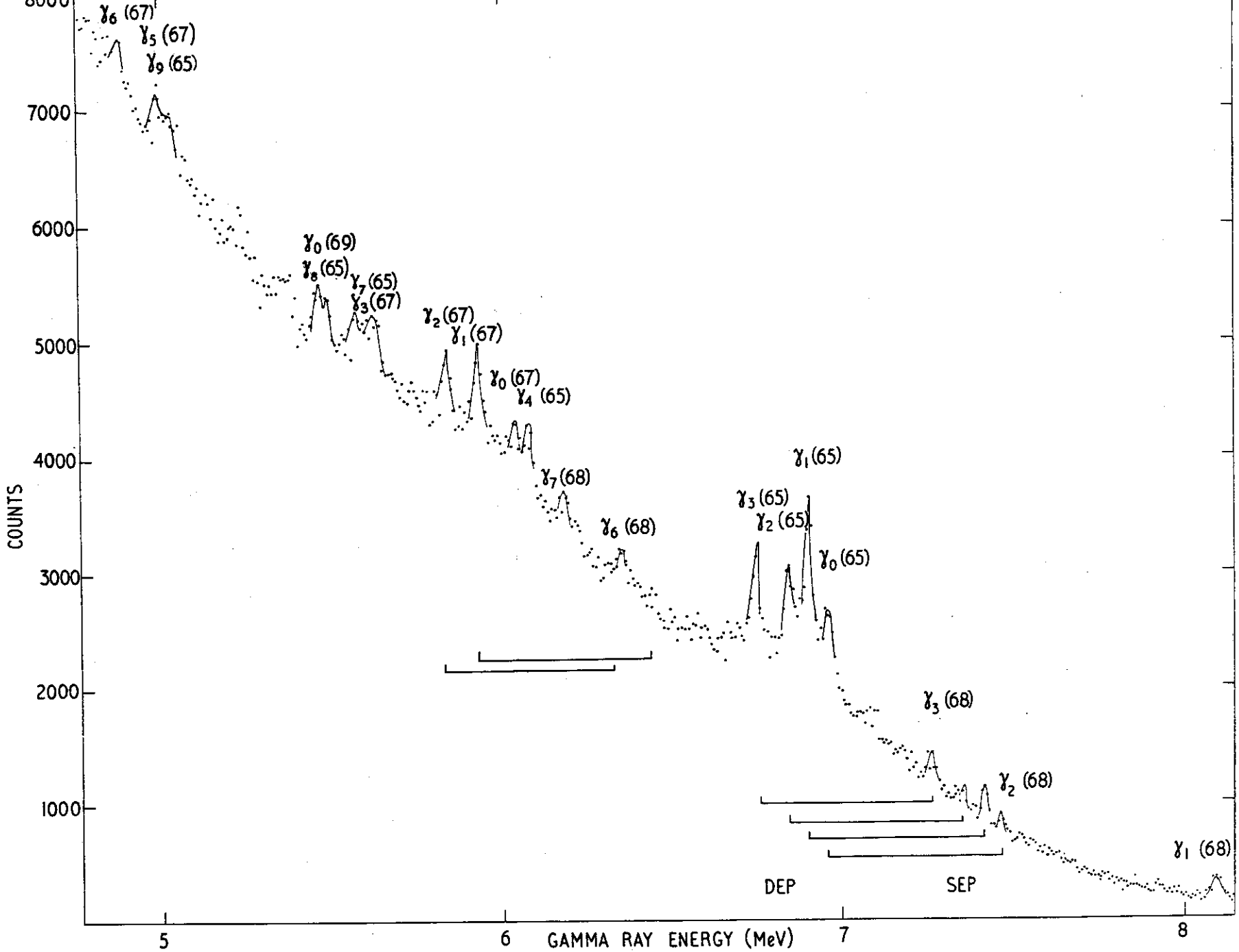

FIGURE 3. '60 keV AVERAGED' SUM SPECTRA IN ZINC

THE BACKGROUND SUBTRACTED SPECTRA ARE SHIFTED IN ENERGY TO OVERLAP THE THERMAL ENERGIES AND THEN ADDED.

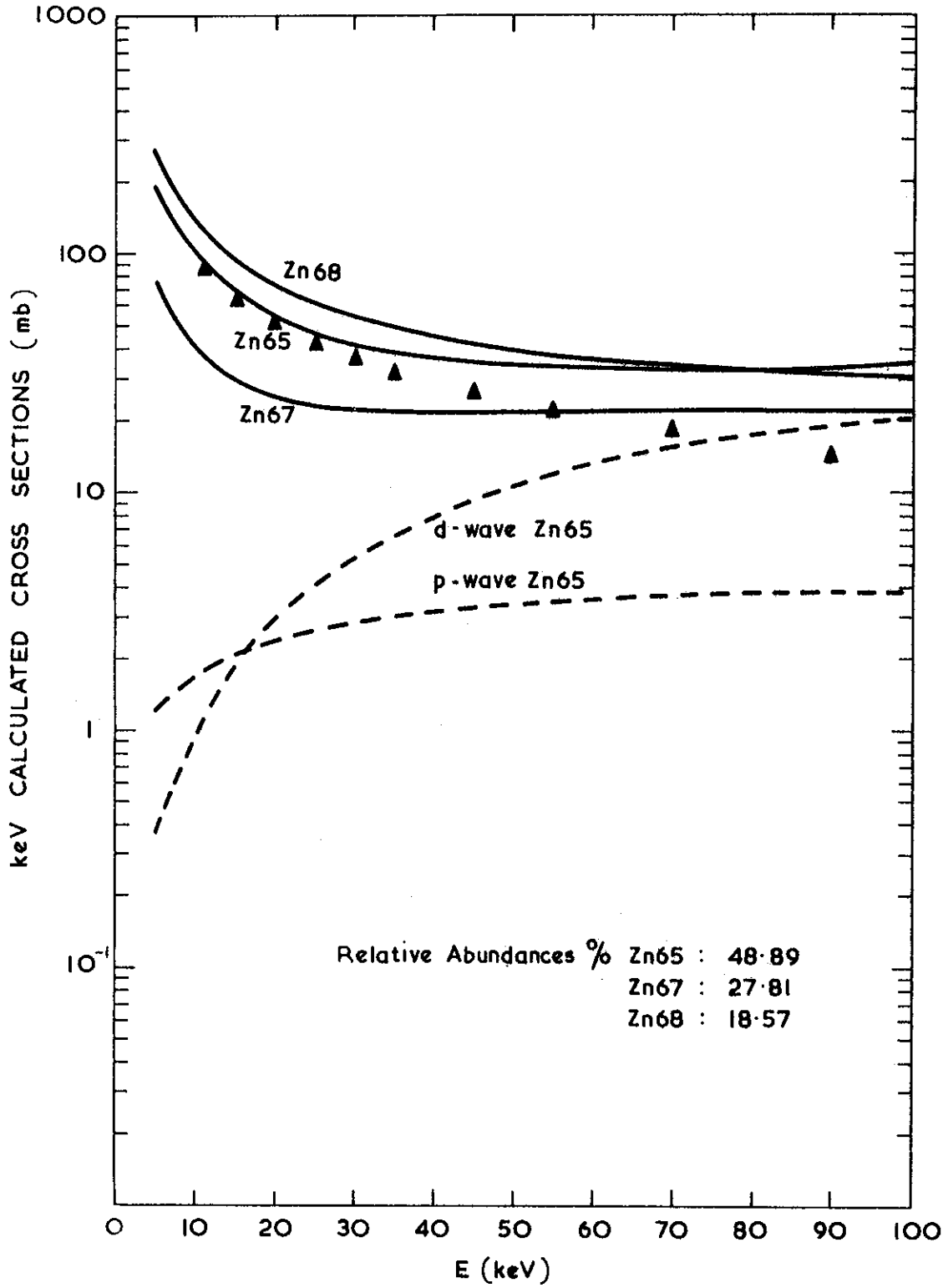

FIGURE 4. ℓ-WAVE CAPTURE CROSS SECTIONS

Calculated keV capture cross sections for zinc isotopes from Musgrove (1969) are shown with the experimental natural zinc cross section of Macklin and Gibbons (1965). The p- and d-wave contributions to the ^{65}Zn cross section are also shown.

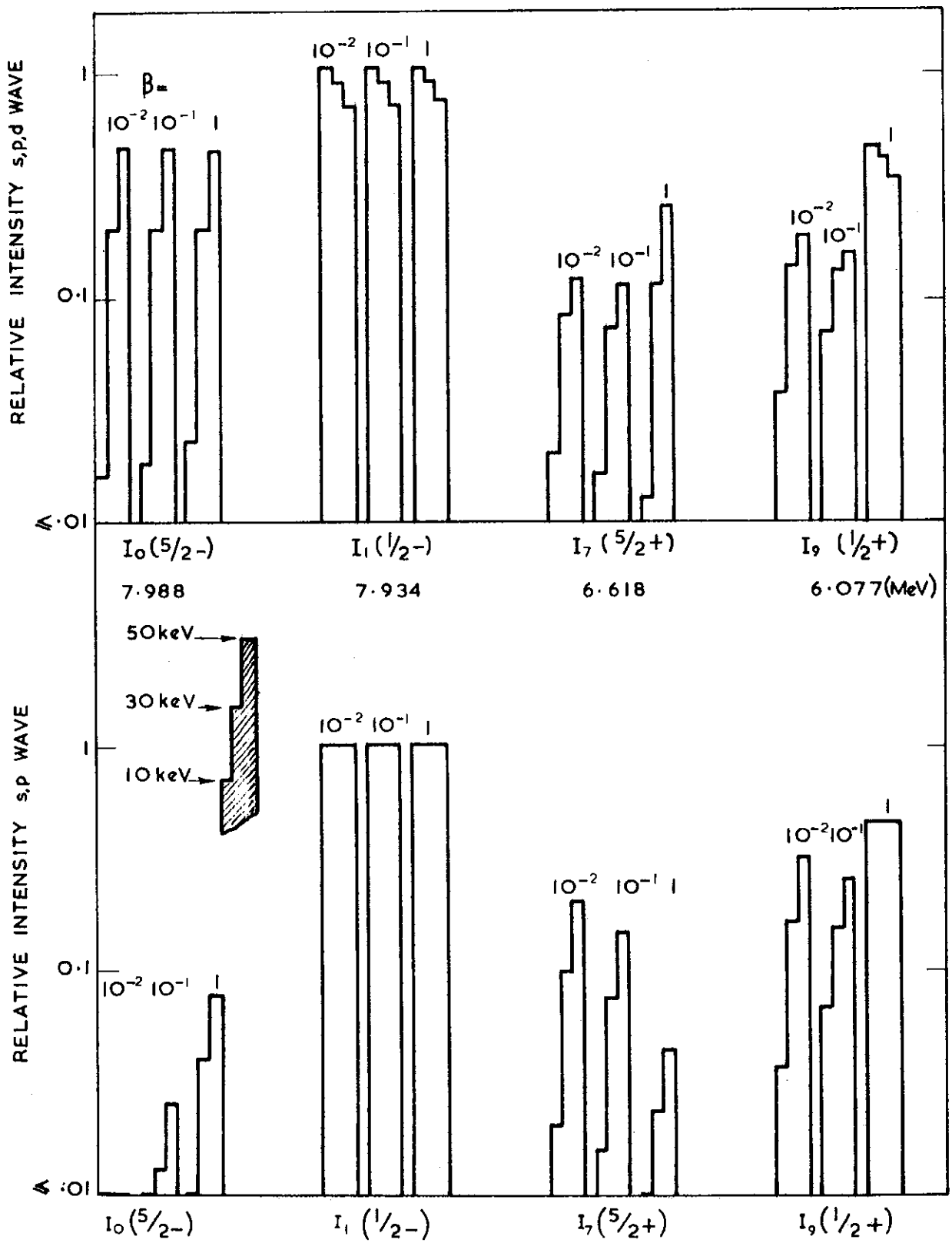

FIGURE 5. GAMMA RAY INTENSITIES CALCULATED FOR A STATISTICAL MODEL REACTION MECHANISM IN ^{65}Zn

Intensities are given for neutron energies of 10, 30 and 50 keV, relative to the second excited state transition (3/2−, E_γ = 7.873 MeV). Results are shown for β = M1/E1 = 0.01, 0.1, 1.0.

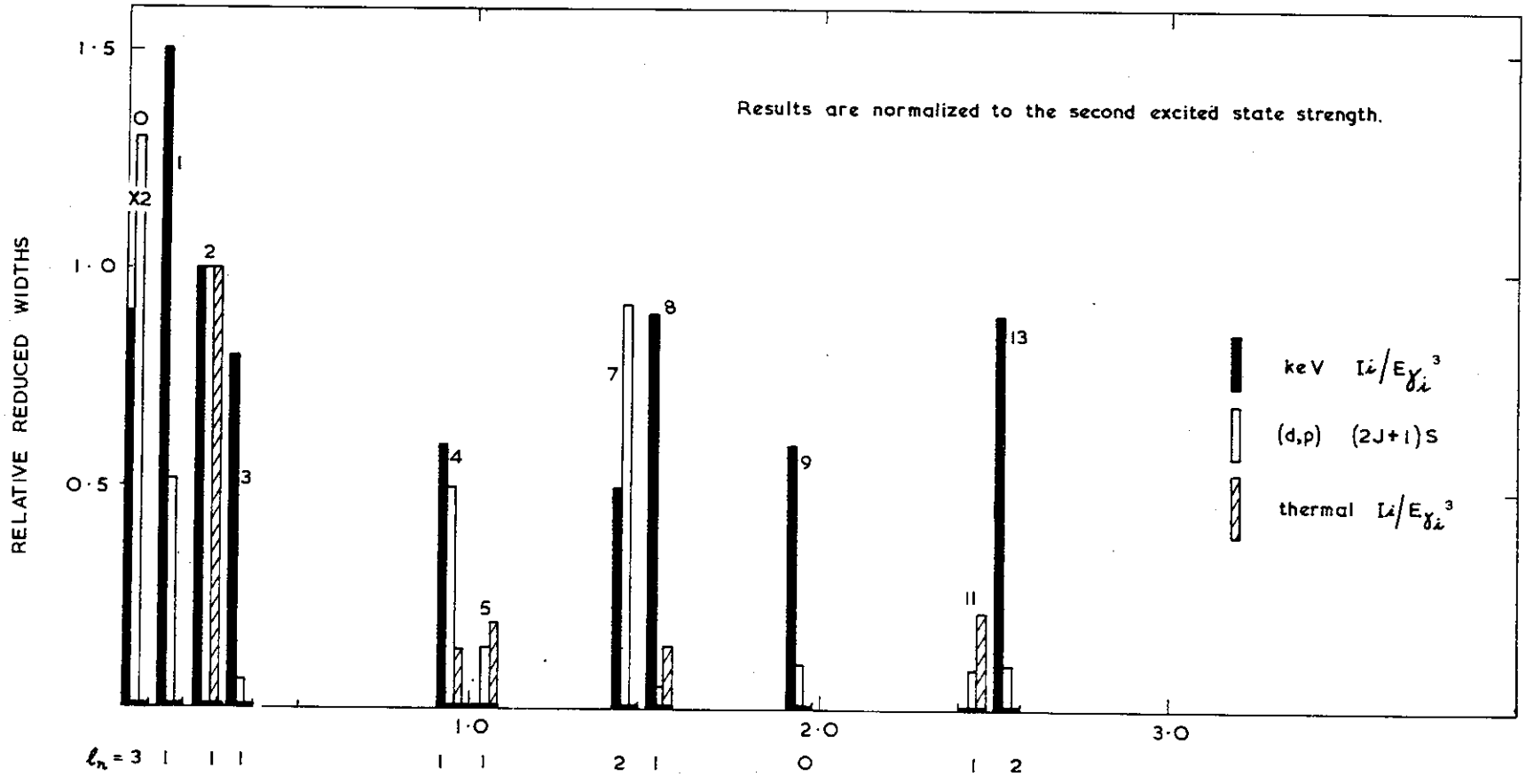

FIGURE 6. COMPARISON OF NEUTRON REDUCED WIDTHS AND GAMMA RAY MATRIX ELEMENTS

Thermal results should be compared with only ℓ_n = 1 neutron widths

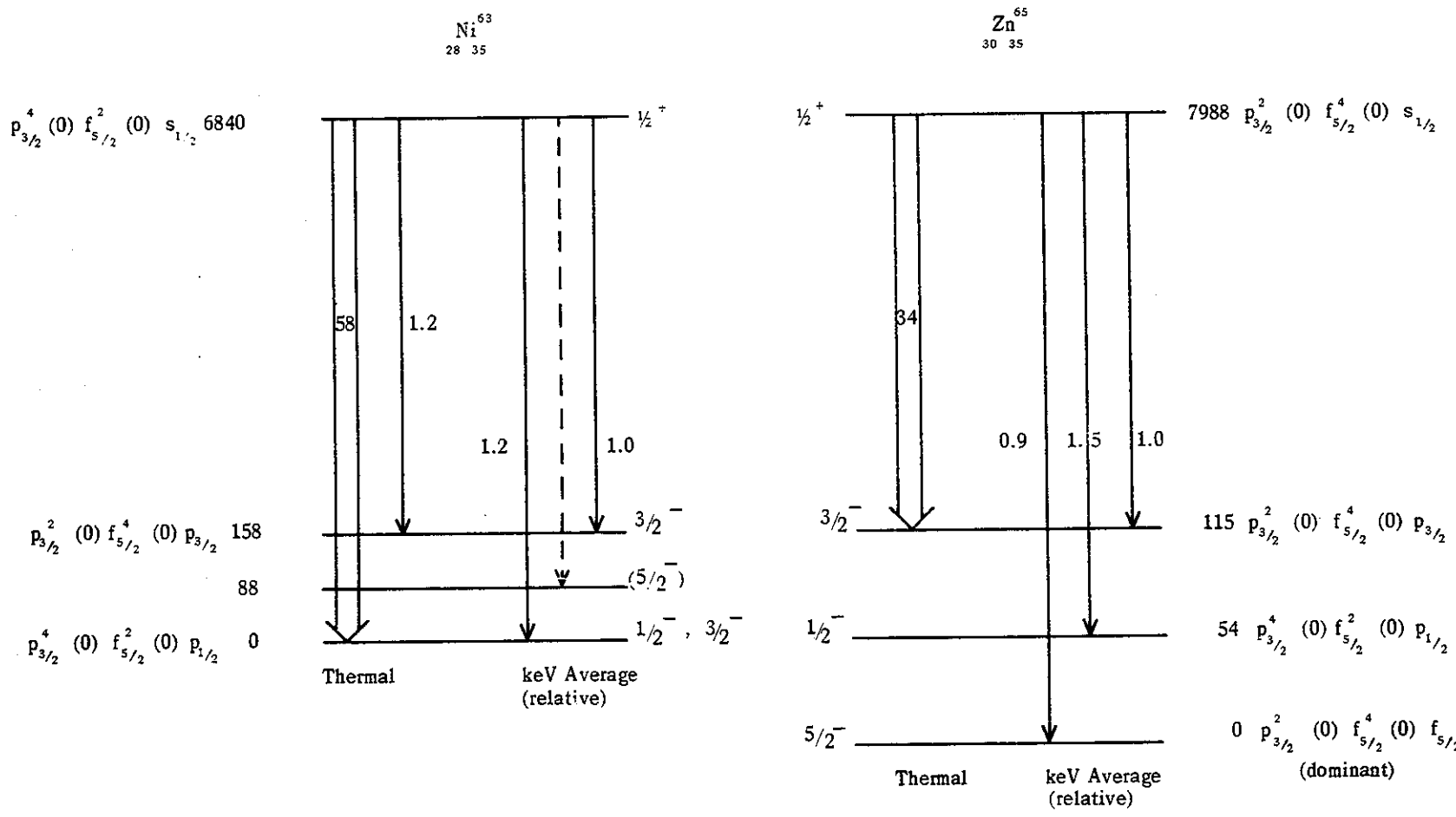

FIGURE 7. NEUTRON CONFIGURATIONS IN ^{63}Ni AND ^{65}Zn

A consistent set of neutron configurations is given for these isotopes to account for the observed capture gamma ray intensities